between the natural frequencies. Separating the natural frequencies, in effect, removes a section along the diagonal $\omega_1 = \omega_2$, as shown in Fig. 4. This leaves behind much of the ridges that extend outward from the diagonal. However, the height of the ridges as seen in Fig. 1 is substantial. Small errors are therefore not insured by just removing a slice along the diagonal. Also, as seen in the figures, only a small portion along the diagonal—which contains the peak—needs to be removed. Instead of frequency separation, it would be more appropriate to remove or avoid regions near the excitation frequencies, as shown in Fig. 5. This approach of frequency avoidance addresses the ridge-like nature of the error. It would remove the ridges and the peak error, while allowing much of the diagonal region to remain intact. Although a limited set of data is presented in this paper, extensive numerical calculations have been performed by the author, and all numerical simulations have yielded qualitatively identical results.

## IV. Conclusions

Given a system under harmonic excitation, the error introduced by the decoupling approximation depends on three parameters. They are the modal damping matrix, the natural frequencies, and the excitation. The approach of frequency separation is not adequate in insuring small errors. Instead, the approach of frequency avoidance provides a more effective method for controlling the error and, thus, for decoupling the system of equations. An analytical formula for the approximation error has also been presented to highlight the effect of the interplay of the three parameters on the approximation error.

## Acknowledgment

This research has been supported in part by the National Science Foundation under Grant MSS-8657619. Opinions, findings, and conclusions expressed in this paper are those of the authors and do not necessarily reflect the views of the National Science Foundation.

## References

[1]Shahruz, S. M., and Ma, F., "Approximation Decoupling of the Equations of Motion of Linear Underdamped Systems," *Journal of Applied Mechanics,* Vol. 55, No. 3, 1988, pp. 716-720.

[2]Hwang, J. H., and Ma, F., "On the Approximate Solution of Nonclassically Damped Linear Systems," *Journal of Applied Mechanics* (to be published).

[3]Hasselman, T. K., "Modal Coupling in Lightly Damped Structures," *AIAA Journal,* Vol. 14, No. 11, 1976, pp. 1627-1628.

[4]Warburton, G. B., and Soni, S. R., "Errors in Response Calculations for Non-Classically Damped Structures," *Earthquake Engineering and Structural Dynamics,* Vol. 5, No. 4, 1977, pp. 365-376.

# Free Vibration Analysis of Rectangular Plates with Free Edges and Line Support Along Diagonals

Nong Li* and D. J. Gorman†
*University of Ottawa,*
*Ottawa, Ontario K1N 6N5, Canada*

## Nomenclature

| | |
|---|---|
| $a,b$ | = dimensions of plate in $\xi$ and $\eta$ direction |
| $D$ | = flexural rigidity of plate, $[Eh^3/12(1-\nu^2)]$ |
| $E$ | = Young's modulus of plate material |
| $h$ | = thickness of plate |
| $K^*$ | = upper subscript limit for first summations of solution |
| $W(\xi,\eta)$ | = amplitude of plate vibration |
| $x,y$ | = plate spatial coordinates |
| $\eta$ | = dimensionless plate spatial coordinate, $y/b$ |
| $\lambda^2$ | $= \omega\, a^2\sqrt{\rho/D}$ |
| $\lambda^{*2}$ | $= \omega\, b^2\sqrt{\rho/D}$ |
| $\nu$ | = Poisson's ratio |
| $\xi$ | = dimensionless plate spatial coordinate, $x/a$ |
| $\rho$ | = mass of plate per unit area |
| $\phi$ | = plate aspect ratio, $b/a$ |
| $\phi_1$ | = inverse of plate aspect ratio, $a/b$ |
| $\omega$ | = circular frequency of vibration |

Received Oct. 14, 1991; revision received Dec. 5, 1991; accepted for publication Dec. 6, 1991. 

*Research Assistant, Department of Mechanical Engineering.
†Professor, Department of Mechanical Engineering.

## Introduction

Although free vibration problems of free rectangular plates and plates with symmetrically distributed point supports on the lateral surface were investigated by Gorman,[1-3] where he used the superposition method to obtain analytical solutions, a review of the literature[4-6] reveals that no study has been made for the problem of free rectangular plates with line support along the diagonals.

It would seem that the title problem would be difficult to solve because of the existence of the line support. However, it will be seen that the superposition method can be utilized to obtain accurate solutions when the line support is replaced by a limited number of equally spaced point supports as described in this paper. Convergence tests show that only 20 point supports and 15 terms in series expansions are sufficient to guarantee rapid convergence to exact eigenvalues.

To save computing time and obtain rapid convergence, all of the vibration modes of this plate are placed in one of the following categories: fully symmetric, fully antisymmetric, or symmetric-antisymmetric modes with respect to the plate central axes. Eigenvalues are tabulated for the first four free vibration modes of plates with a wide range of plate geometries.

## Mathematical Procedure

Consider the rectangular plate as shown in Fig. 1. The plate is of dimensions $2a \times 2b$ and has free edge conditions along all boundaries. In addition, the plate is subjected to internal line support along its diagonals, where lateral displacements are forbidden, but no bending moments normal to the line of support are imparted to the plate.

It is appreciated that the line support can be replaced by point supports, provided that the number of points are large enough to forbid lateral motion along the diagonals. This condition will be easily realized by imposing zero displacement at each of the points.

Since all modes must be symmetric with respect to the $\xi$ and $\eta$ axes and antisymmetric with respect to the $\xi$ and $\eta$ axes or symmetric with respect to the $\xi$ (or $\eta$) axis and antisymmetric with respect to $\eta$ (or $\xi$) axis, only one quarter of the plate needs

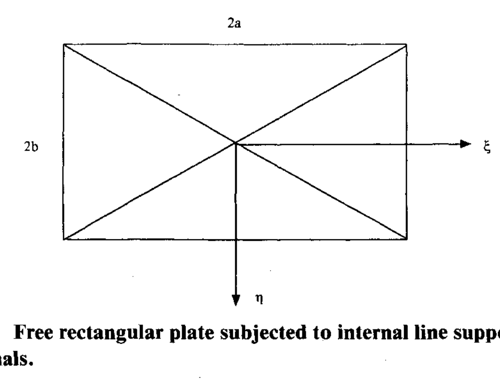


**Fig. 1 Free rectangular plate subjected to internal line support along diagonals.**

to be analyzed. On the other hand, because the analysis procedures are almost the same for each family of modes, analysis of the fully symmetric modes only will be discussed here.

The quarter section of the original plate and the three building blocks for analyzing this family of vibration modes are shown in Fig. 2. The small pairs of circles adjacent to the edges imply slip shear conditions (i.e., zero vertical edge reaction and zero slope). To avoid *rejection modes*,[7] distributed harmonic rotations are imposed along the edge $\eta = 1$ of the first building block and the edge $\xi = 1$ of the second block, respectively.

The solution for the first building block is easily obtained by following procedures as described in Ref. 7 and the amplitude of distributed rotation is expanded in the series

$$\left.\frac{\partial W_1(\xi,\eta)}{\partial \eta}\right|_{\eta=1} = \sum_{m=0,1}^{\infty} E_m \cos m\pi\xi \tag{1}$$

Because of the similarity between the first two building blocks, the solution for $W_2(\xi,\eta)$ can be easily extracted from the first by replacing $\phi$ of the first solution with its inverse $\phi_1$ and $\lambda^2$ with $\lambda^2\,\phi^2$.

Next consider the solution $W_3(\xi,\eta)$ for the third building block. Since the line support is considered to act as a sequence of point supports one may write

$$W_3(\xi,\eta) = \sum_{i=1,2}^{K_p} W_i^*(\xi,\eta) \tag{2}$$

where $K_p$ is the number of point supports and $W_i^*(\xi,\eta)$ is the solution associated with the $i$th point support at which a concentrated harmonic force of magnitude $P_i$ and circular frequency $\omega$ acts. Dimensionless coordinates of the $i$th point support are $(\eta_i,\eta_i)$. The force can be expanded in a cosine series as

$$P_i(\xi) = \sum_{m=0,1}^{\infty} P_i^* \cos m\pi\eta_i \cos m\pi\xi \tag{3}$$

where

$$P_i^* = -2P_i b^3/Da^2\delta$$

$$\delta = \begin{cases} 2 \text{ if } m = 0 \\ 1 \text{ if } m \neq 0 \end{cases}$$

The solution for $W_i^*(\xi,\eta)$ is expressed[3] for $\eta \le \eta_i$

$$W_i^*(\xi,\eta) = \sum_{m=0,1}^{K^*} (A_{im}\cosh\beta_m\eta + B_{im}\cos\gamma_m\eta)\cos m\pi\xi + \sum_{m=K^*+1}^{\infty} (A_{im}\cosh\beta_m\eta + B_{im}\cosh\gamma_m\eta)\cos m\pi\xi \tag{4}$$

and for $\eta > \eta_i$

$$W_i^*(\xi,\eta) = \sum_{m=0,1}^{K^*} (C_{im}\cosh\beta_m\eta^* + D_{im}\cos\gamma_m\eta^*)\cos m\pi\xi + \sum_{m=K^*+1}^{\infty} (C_{im}\cosh\beta_m\eta^* + D_{im}\cosh\gamma_m\eta^*)\cos m\pi\xi \tag{5}$$

where $\eta^* = 1-\eta$ and the four constants $A_{im}$, $B_{im}$, $C_{im}$, and $D_{im}$ are determined by the conditions of continuity of displacement, slope, bending moment, and vertical reaction along the interface $\eta = \eta_i$ as described in Ref. 3. They are not reproduced here in the interest of saving space.

The eigenvalue matrix is obtained by requiring that bending moments must vanish along the edges $\xi = 1$ and $\eta = 1$ of the combined solutions. In addition, we require that net lateral displacement must equal zero at each support point.

## Presentation of Computed Results

Before examining the computed eigenvalues, it is necessary to carry out a convergence test that will determine how many point supports need to be used and how many terms are to be taken in the series expansions to guarantee accuracy of the computed eigenvalues. Typical convergence test results are shown in Table 1 for the second fully symmetric vibration mode of a square plate. It is seen that the eigenvalue converges

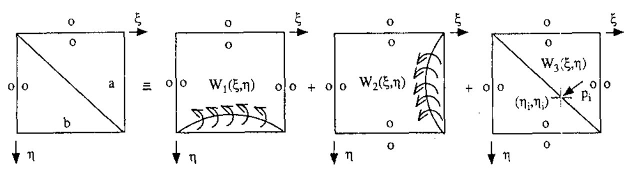


**Fig. 2 Building blocks for analyzing the fully symmetric vibration modes of the plate.**

**Table 1 Results of convergence test for second fully symmetric mode of square plate ($\lambda^2 = \omega a^2\sqrt{\rho/D}$)**

| | $K$[a] | | | | |
|---|---|---|---|---|---|
| $K_p$[b] | 10 | 12 | 14 | 16 | 20 |
| 10 | 14.4304 | 14.4280 | 14.4273 | 14.4268 | 14.4252 |
| 12 | 14.4345 | 14.4328 | 14.4321 | 14.4317 | 14.4304 |
| 14 | 14.4359 | 14.4348 | 14.4339 | 14.4338 | 14.4328 |
| 16 | 14.4364 | 14.4355 | 14.4349 | 14.4348 | 14.4340 |
| 18 | 14.4367 | 14.4358 | 14.4354 | 14.4352 | 14.4346 |
| 20 | 14.4368 | 14.4360 | 14.4356 | 14.4354 | 14.4349 |
| 25 | 14.4369 | 14.4362 | 14.4358 | 14.4357 | 14.4354 |

[a]Number of terms in series. [b]Number of point supports.

**Table 2 First four eigenvalues for fully symmetric vibration modes ($\lambda^2 = \omega a^2\sqrt{\rho/D}$)**

| | $\phi = b/a$ | | | | | | | | |
|---|---|---|---|---|---|---|---|---|---|
| Mode | 1.0 | 1.25 | 1.5 | 1.75 | 2.0 | 2.25 | 2.5 | 2.75 | 3.0 |
| 1 | 4.860 | 4.083 | 3.837 | 3.745 | 3.703 | 3.674 | 3.646 | 3.620 | 3.588 |
| 2 | 14.44 | 11.16 | 8.835 | 7.321 | 6.333 | 5.674 | 5.221 | 4.903 | 4.676 |
| 3 | 29.11 | 24.66 | 22.82 | 19.01 | 15.64 | 13.29 | 11.59 | 10.34 | 9.394 |
| 4 | 39.97 | 31.11 | 23.99 | 21.62 | 20.37 | 18.85 | 17.09 | 15.37 | 13.86 |

**Table 3 First four eigenvalues for fully antisymmetric vibration modes ($\lambda^2 = \omega a^2\sqrt{\rho/D}$)**

| | $\phi = b/a$ | | | | | | | | |
|---|---|---|---|---|---|---|---|---|---|
| Mode | 1.0 | 1.25 | 1.5 | 1.75 | 2.0 | 2.25 | 2.5 | 2.75 | 3.0 |
| 1 | 17.03 | 14.10 | 12.59 | 11.60 | 10.80 | 10.08 | 9.448 | 8.904 | 8.444 |
| 2 | 31.48 | 24.46 | 19.68 | 16.75 | 15.00 | 13.97 | 13.34 | 12.93 | 12.65 |
| 3 | 50.64 | 42.52 | 36.73 | 30.31 | 25.35 | 21.79 | 19.19 | 17.25 | 15.75 |
| 4 | 72.40 | 54.37 | 44.52 | 41.00 | 38.39 | 34.03 | 29.72 | 26.31 | 23.65 |

Table 4 First four eigenvalues for symmetric-antisymmetric vibration modes ($\lambda^2 = \omega a^2 \sqrt{\rho/D}$)

| | $\phi = b/a$ | | | | | | | | |
|---|---|---|---|---|---|---|---|---|---|
| Mode | 1.0 | 1.25 | 1.5 | 1.75 | 2.0 | 2.25 | 2.5 | 2.75 | 3.0 |
| 1 | 8.875 | 7.945 | 7.288 | 6.768 | 6.354 | 6.027 | 5.765 | 5.554 | 5.372 |
| 2 | 23.68 | 18.43 | 15.71 | 14.24 | 13.37 | 12.78 | 12.31 | 11.84 | 11.32 |
| 3 | 36.68 | 31.92 | 26.57 | 22.02 | 18.78 | 16.50 | 14.92 | 13.85 | 13.17 |
| 4 | 48.04 | 39.80 | 35.38 | 33.02 | 31.14 | 27.77 | 24.31 | 21.63 | 19.55 |

Table 5 First four eigenvalues for symmetric-antisymmetric vibration modes ($\lambda^{*2} = \omega b^2 \sqrt{\rho/D}$)

| | $\phi_1 = a/b$ | | | | | | | | |
|---|---|---|---|---|---|---|---|---|---|
| Mode | 1.0 | 1.25 | 1.5 | 1.75 | 2.0 | 2.25 | 2.5 | 2.75 | 3.0 |
| 1 | 8.875 | 6.552 | 5.355 | 4.697 | 4.310 | 4.066 | 3.901 | 3.781 | 3.690 |
| 2 | 23.68 | 19.44 | 15.65 | 12.76 | 10.74 | 9.335 | 8.328 | 7.589 | 7.034 |
| 3 | 36.68 | 27.62 | 23.79 | 21.44 | 19.02 | 16.58 | 14.51 | 12.87 | 11.57 |
| 4 | 48.04 | 37.71 | 31.41 | 26.94 | 24.00 | 22.05 | 20.46 | 18.70 | 16.94 |

very quickly, and 20 point supports and 15 terms are enough to guarantee accuracy up to 4 digits. Therefore, it was decided to set the number of point supports $K_p$ equal to 20 and the number of terms in the expansion $K$ equal to 15 for all of the computed eigenvalues.

All of the results presented here are computed with a value of Poisson's ratio equal to 0.333. The first four eigenvalues for fully symmetric and fully antisymmetric vibration modes are given in Tables 2 and 3, where the aspect ratio $\phi$ varies between 1 and 3. In Tables 4 and 5 corresponding eigenvalues are tabulated for the symmetric-antisymmetric vibration modes, where the aspect ratio is allowed to vary from 1/3 to 3 because of nonsymmetry of this family of modes.

It should be pointed out that some eigenvalues for the title plate can be established in advance. For instance, the first eigenvalue, 4.806, of fully symmetric modes of the square plate ($\phi = 1$) in Table 2 is equal to the first eigenvalue for fully symmetric modes of free square plates.[1] This is because there are naturally two nodal lines along the diagonals for the mode shape of the latter, independently of whether the line support exists. Accordingly, the third and the fourth eigenvalues of square plates in Table 2 coincide with the fourth and the sixth of the associated modes of fully free plates. Those eigenvalues are usually called *inactive support eigenvalues* since in those cases the line support has no effect on the frequencies and mode shapes.

## Conclusion

The superposition method is a very efficient tool for plate vibration analysis. This technique, with some modification to include line support, has successfully solved the title problem. Convergence is found to be rapid and the accuracy of frequencies is high. It is obvious that the analytical technique can be utilized for plates where the line support is given any configuration on the surface. It is hoped that the eigenvalues presented here will be useful to engineers for design purposes and to researchers for checking their findings.

## References

[1]Gorman, D. J., "Free Vibration Analysis of the Completely Free Rectangular Plate by the Method of Superposition," *Journal of Sound and Vibration*, Vol. 57, No. 3, 1978, pp. 437-447.

[2]Gorman, D. J., "Free Vibration Analysis of Rectangular Plates with Symmetrically Distributed Point Supports Along the Edges," *Journal of Sound and Vibration*, Vol. 73, No. 4, 1980, pp. 563-574.

[3]Gorman, D. J., "An Analytical Solution for the Free Vibration Analysis of Rectangular Plates Resting on Symmetrically Distributed Point Supports," *Journal of Sound and Vibration*, Vol. 79, No. 4, 1981, pp. 561-574.

[4]Leissa, A. W., "Recent Research in Plate Vibration, 1973-1976: Complicating Effects," *Shock and Vibration Digest*, Vol. 10, No. 12, 1978, pp. 21-35.

[5]Leissa, A. W., "Plate Vibration Research, 1976-1980: Complicating Effects," *Shock and Vibration Digest*, Vol. 13, No. 10, 1981, pp. 19-36.

[6]Leissa, A. W., "Recent Studies in Plate Vibrations, 1981-1985, Part II: Complicating Effects," *Shock and Vibration Digest*, Vol. 19, No. 3, 1987, pp. 10-24.

[7]Gorman, D. J., *Free Vibration Analysis of Rectangular Plates*, Elsevier, New York, 1982, Chap. 4.

# Vibration and Buckling of Laminated Plates with a Cutout in Hygrothermal Environment

K. S. Sai Ram* and P. K. Sinha†
*Indian Institute of Technology,*
*Kharagpur 721302, India*

## Introduction

RECENTLY, fiber reinforced plastic composites have been receiving more attention from scientists, engineers, and designers due to their superior properties. They are finding increased application in aerospace and other industries. Since polymer resin is used as a binding material, they are susceptible to environmental effects. Moisture and temperature have a significant effect on the performance of laminated plates due to the introduction of residual stresses, in addition to degradation in their elastic properties. The presence of a cutout further influences the strength and stiffness.

Of late, there is a growing interest to investigate various aspects of composite materials in hygrothermal environment.[1] The effects of moisture and temperature on the free vibration and buckling of laminated plates without a cutout have been considered earlier by the authors.[2,3] Virtually, there is no literature concerning the vibration and buckling of laminated plates with a cutout in hygrothermal environment. Chang and Shio[4] studied thermal buckling of isotropic and composite plates with a hole. A closed-form solution is presented for thermal buckling analysis of an annular isotropic plate with a circular hole, and finite element analysis is used to analyze composite plates with a circular cutout. Numerical results are shown for antisymmetric angle-ply laminates. Reddy[5] investigated large-amplitude flexural vibrations of composite plates with a square cutout using a finite element method. Results are

Received Oct. 21, 1991; revision received Jan. 27, 1992; accepted for publication Jan. 27, 1992. 

*Research Student, Department of Aerospace Engineering.
†Professor, Department of Aerospace Engineering.